Supporting Information

Cell membrane-coated MOF nanocarrier combining CDT for inhibition of hepatocellular carcinoma proliferation and metastasis

Huaying Xie [1, †], Xuhua Xiao [2, †], Xiaoyuan Yi[1], Kunzhao Huang[1], Qingyu Zeng[1], Feifei He[2], Liyan Wang[2, *]

1   The First School of Clinical Medicine, Guilin Medical University, Guilin 541000, P.R. China.

2   Department of Gastroenterology, Affiliated Hospital of Guilin Medical University, Guilin 541000, P.R. China.

*   Correspondence: 168wangliyan@163.com; Tel.: 15295953938.

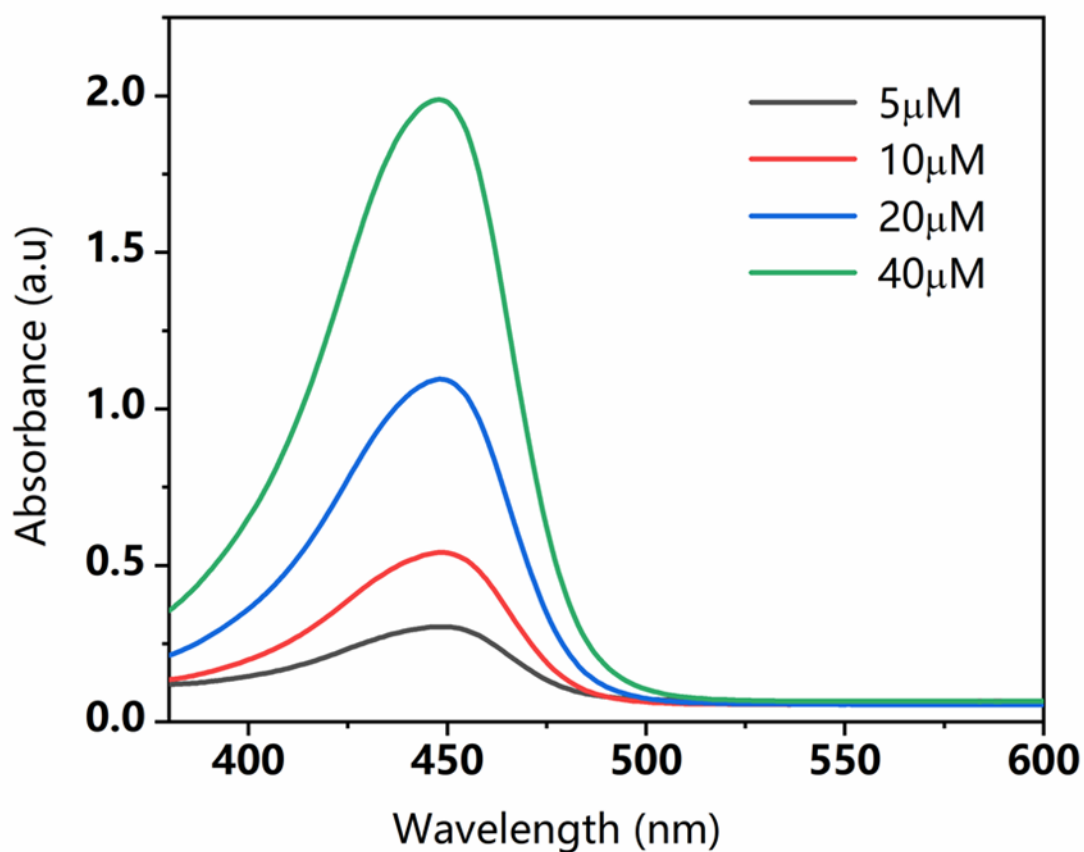†   These authors contributed equally to this work.

Figure S1. UV-vis absorption spectra of ACF in H_2O solution at different concentrations.

$$y = 0.0314x + 0.052$$
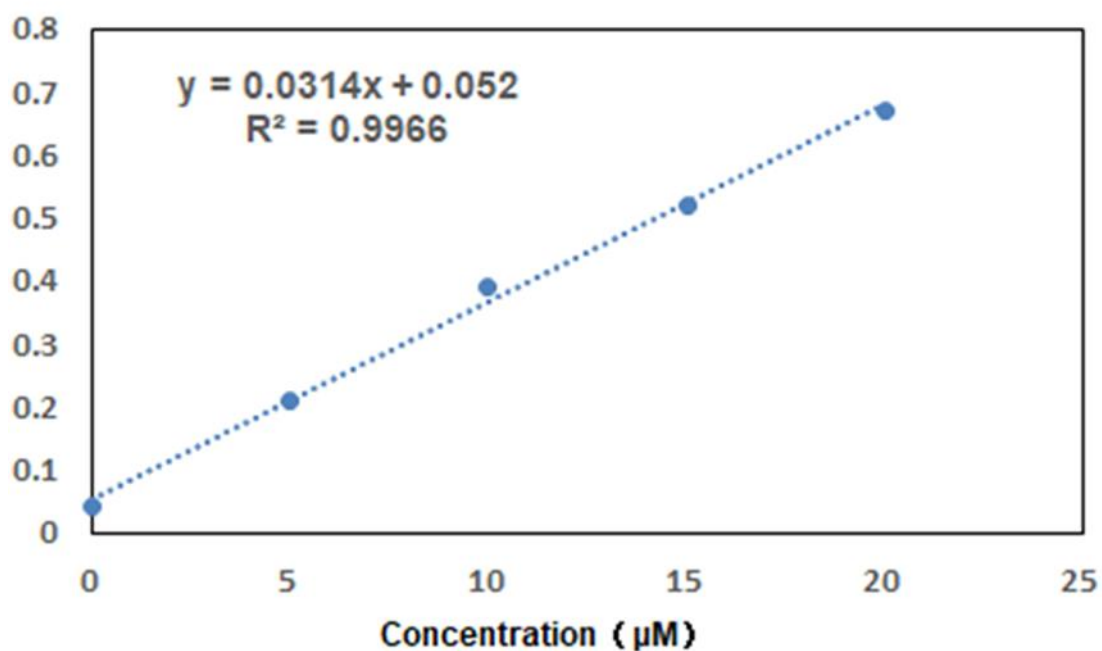$$R^2 = 0.9966$$

Figure S2. The linearly fitted standard curve of ACF characteristic absorption intensity at 460 nm vs concentration.
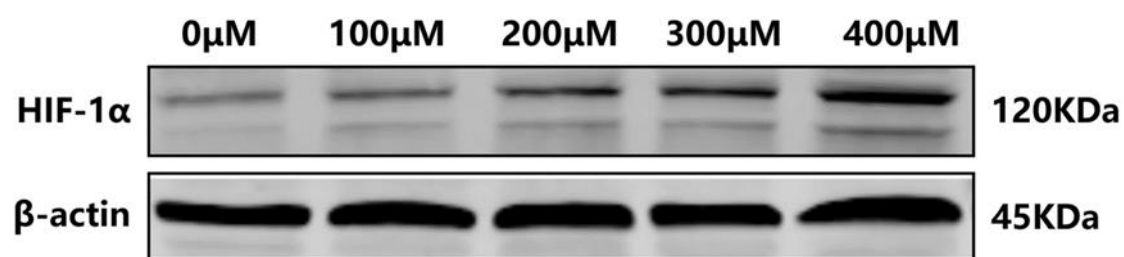
Figure S3. Western blot bands of hypoxia-related proteins (i.e., HIF-1α) in Hepa1-6 cells after incubating with CoCl$_2$ with varied concentrations.
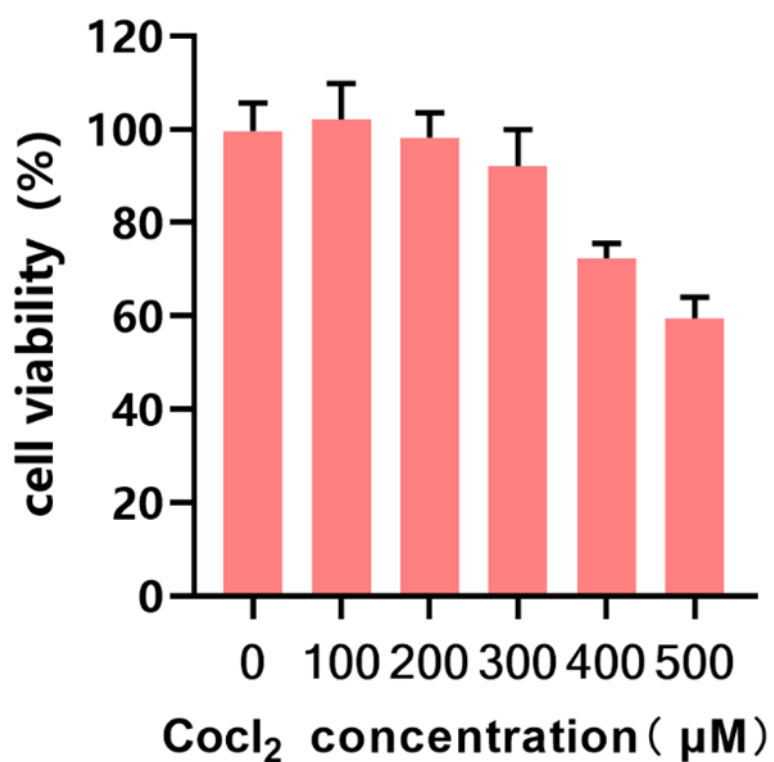

Figure S4. Cell viability of Hepa1-6 cells after incubating with CoCl$_2$ with varied concentrations.
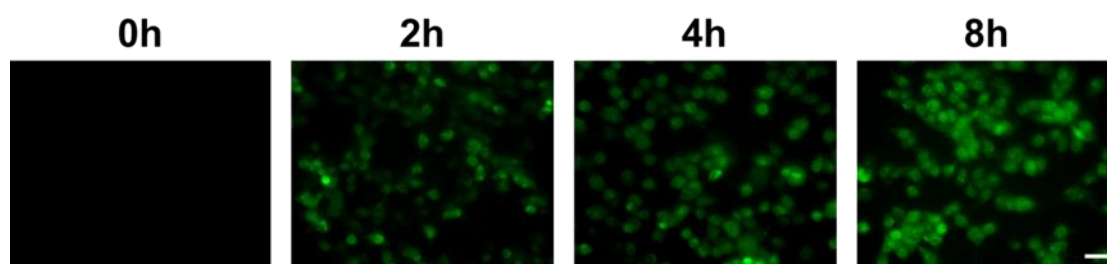
Figure S5. Cell internalization of MIL-101/ACF@CCM nanoagents by Hepa1-6 cells.
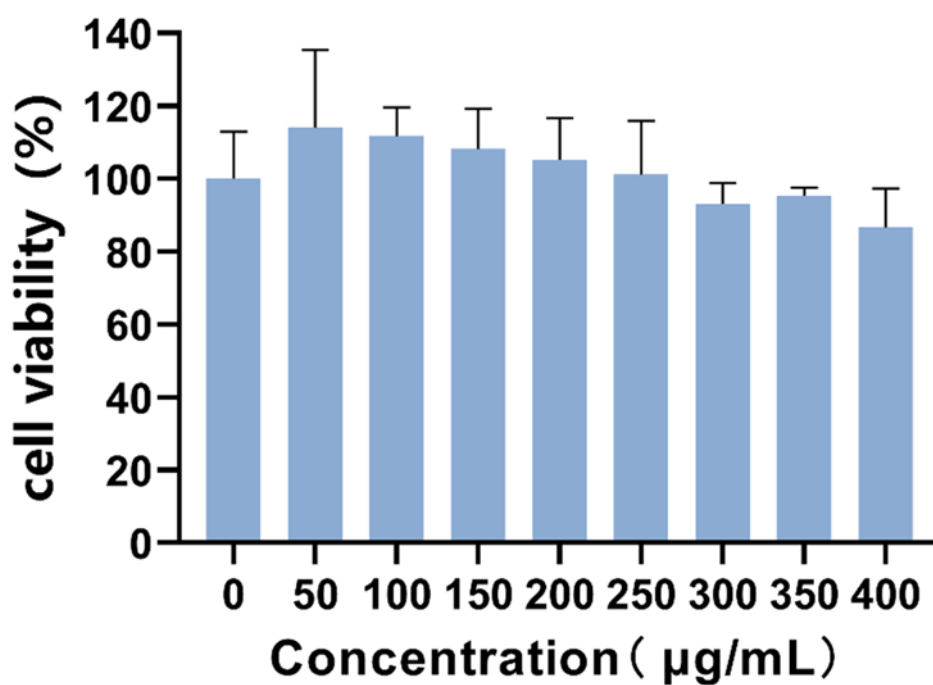
Scale bar: 50 μm.

Figure S6. Cell viabilities of THLE-2 cells after incubation with varied concentrations of MIL-101/ACF@CCM nanoagents for 24 h.
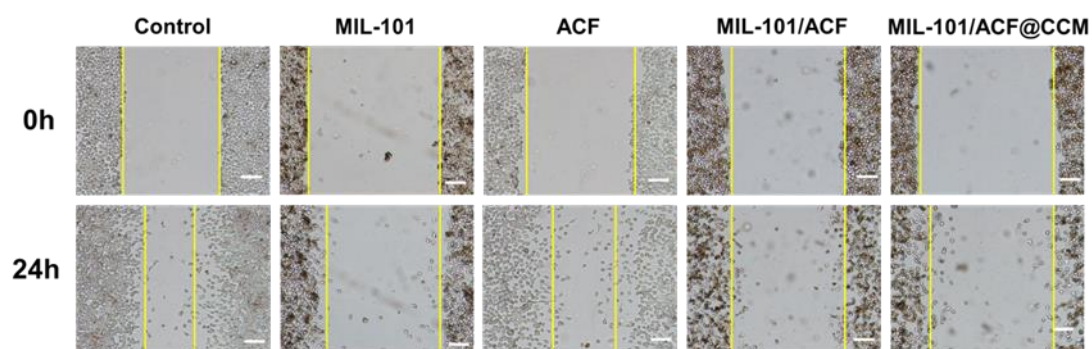
Figure S7. Images of wound healing of hypoxic Hepa1-6 cells after different treatments.
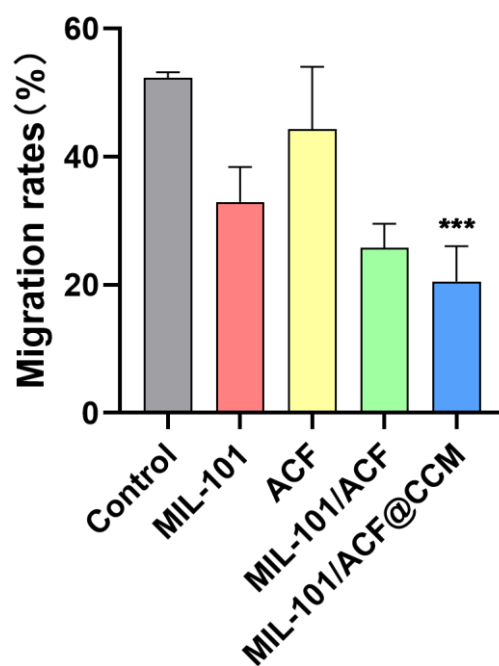

Figure S8. Statistical graph of cell migration distance obtained according to Figure S7. n=3. ***$p < 0.001$.
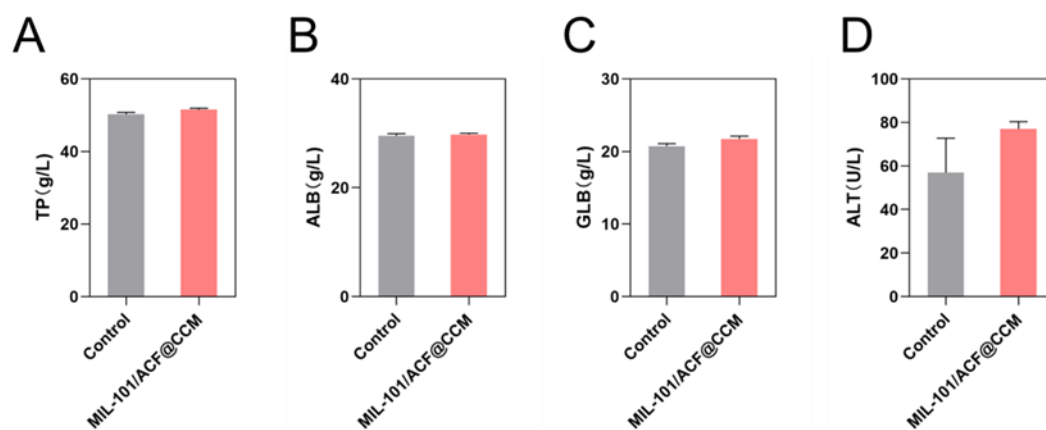
Figure S9. Serum biochemistry assay of mice injected with or without MIL-101/ACF@CCM.
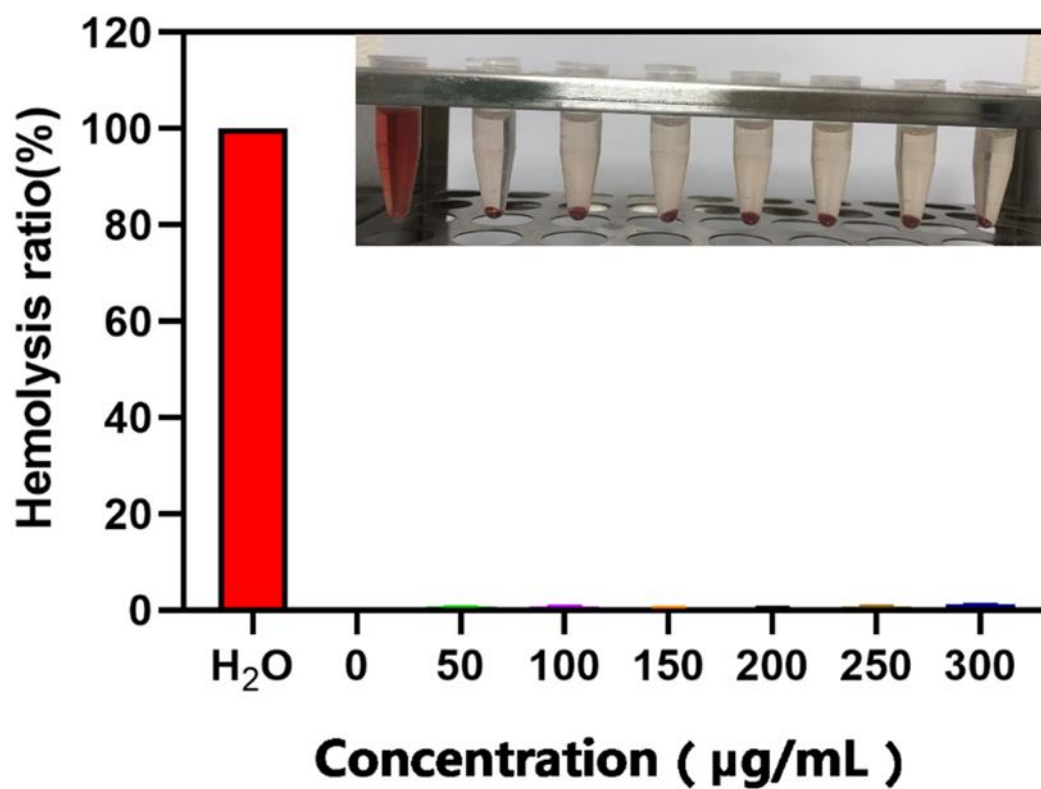

Figure S10. In vitro hemolysis with different concentrations of MIL-101/ACF@CCM.
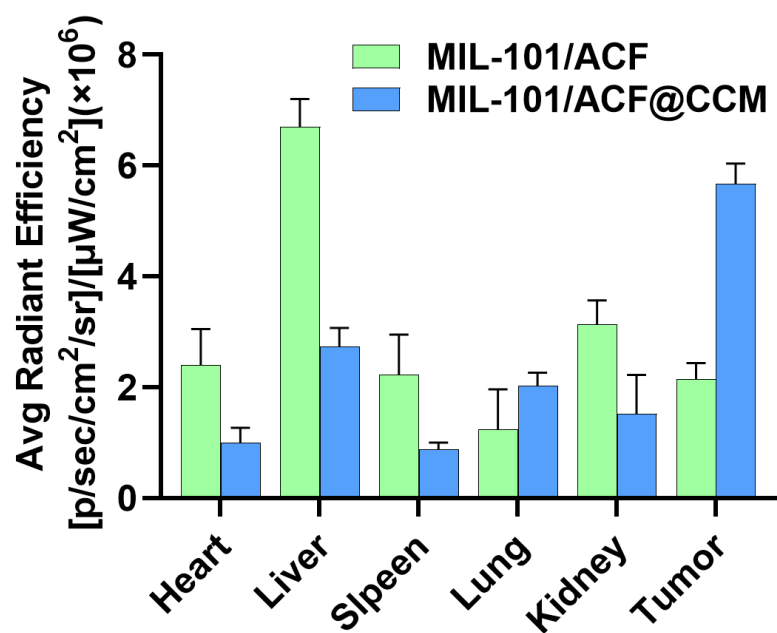
Figure S11. The quantitation of fluorescence from each organ ex vivo (n = 3).
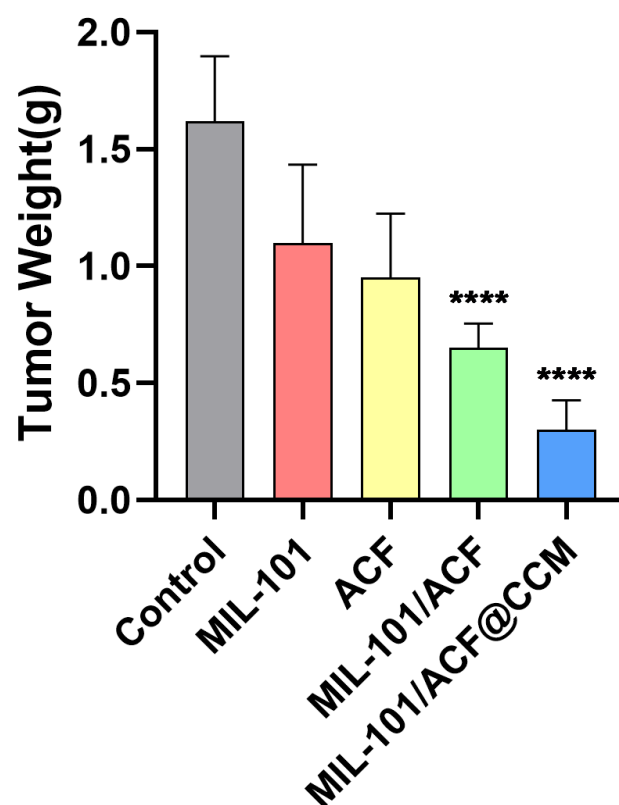

Figure S12. The tumor weights of excised tumors at the end of treatment after (n = 6). ****$p < 0.0001$.